

Phase Separation of Binary Mixtures Induced by Soft Centrifugal Fields

Thomas Zemb¹, Rose Rosenberg², Stjepan Marčelja³, Dirk Haffke², Jean-François Dufrêche¹,
Werner Kunz⁴, Dominik Horinek⁴, Helmut Cölfen²

1 Institute for separation chemistry ICSM U Montpellier/CEA/CNRS/ENSCM, Marcoule, France

2 Physical Chemistry, Department of Chemistry, University of Konstanz, Universitätsstr. 10, D-78457 Konstanz

3 Applied Maths, RSPhys, ANU, ACT 2601, Canberra, Australia

4 Institute of Physical and Theoretical Chemistry, University of Regensburg, D-93040 Regensburg

Supplementary information

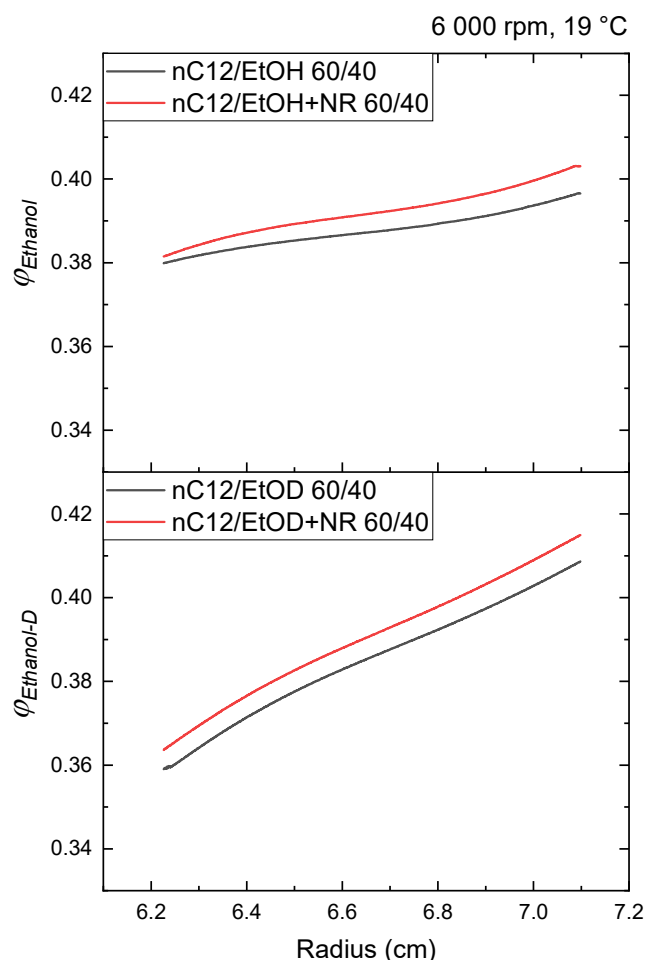


Figure S1: Close to the critical point: Demonstration that there is only a small shift in ethanol concentration, but not in composition gradients, when the dye is added to the composition of H-ethanol (top) and D-ethanol (bottom) near to the critical point.

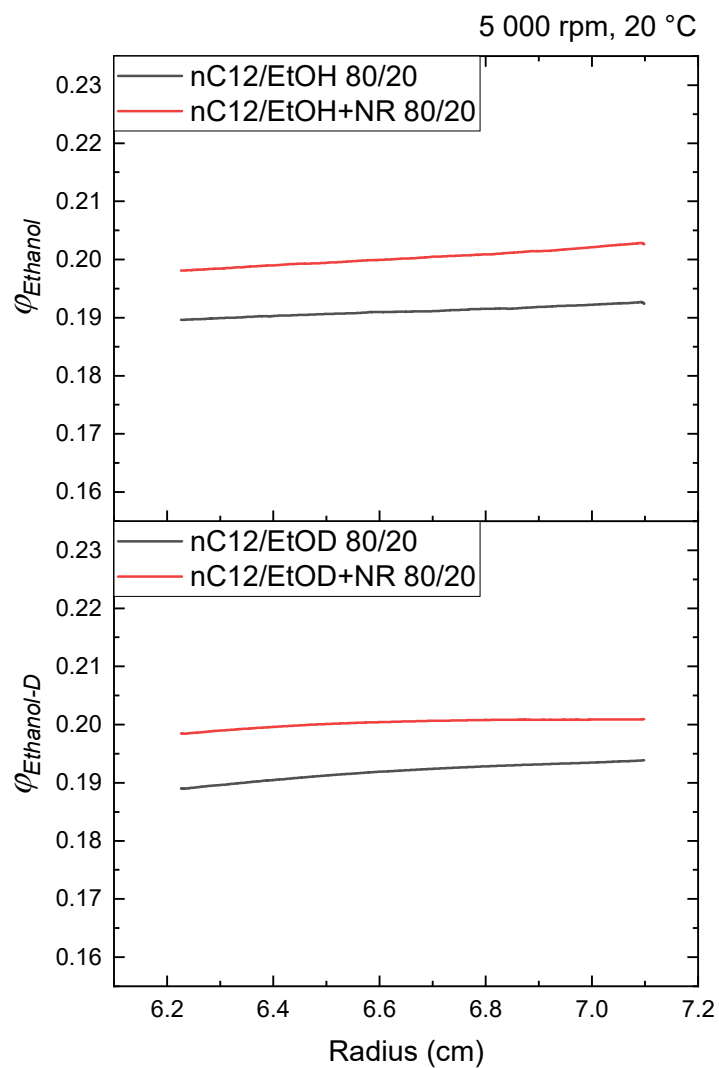


Figure S2: Far from the critical point: this figure shows that the presence of Nile red dye does not affect appreciably the gradients expressed in ethanol volume fraction of 0.20 for H-ethanol (top) and D-ethanol (bottom).

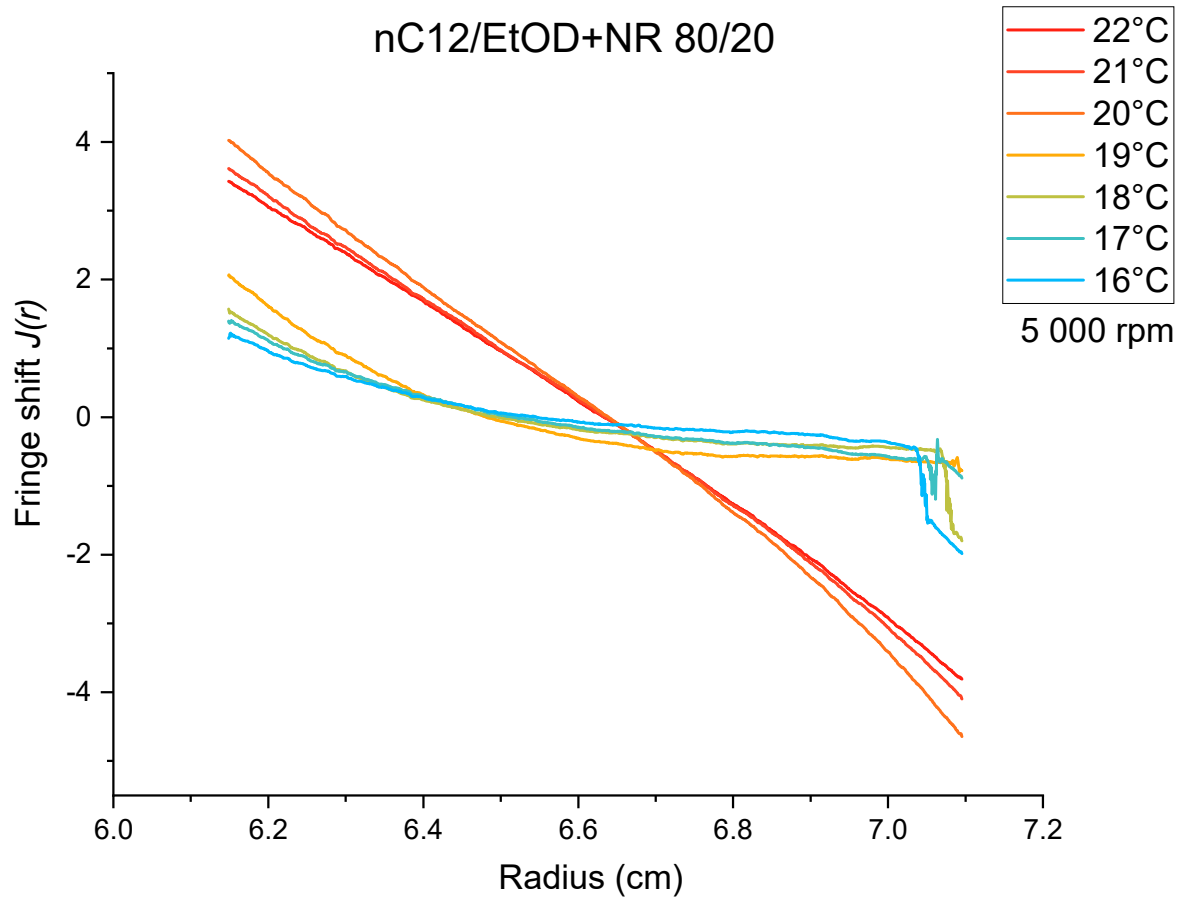


Figure S3: The same experiment as the one shown in figure 3 in the main text, but this time shown as number of fringes: the presence of the dye does *not* affect measurably the gradients and turbidity zones observed when approaching the demixing temperature, even when very far in composition (one third of ethanol content) from the critical point.

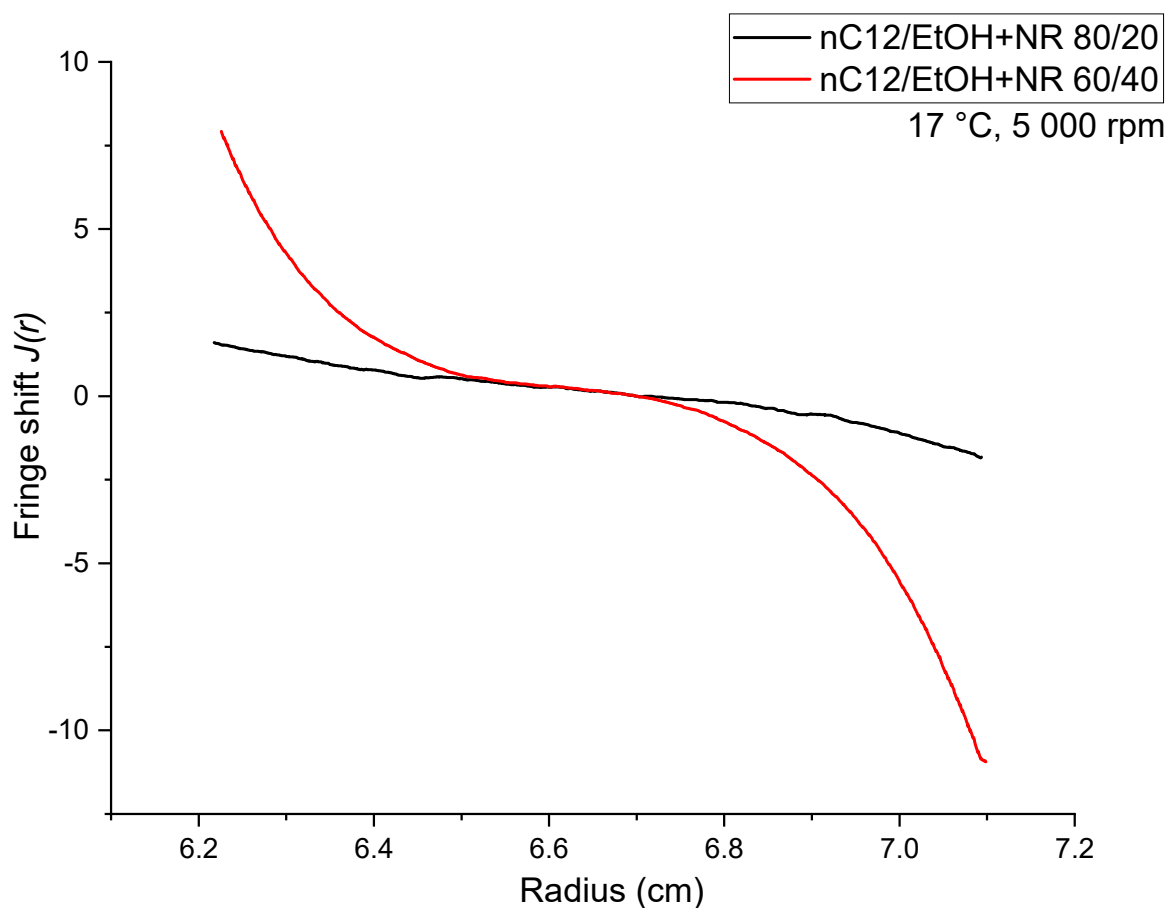


Figure S4: Comparison of the composition gradients expressed in number of fringes obtained in single phase fluids 2 °C above the phase transition temperature T_s for “close” (40 % of ethanol mass fraction) and 5 °C above the T_s for “far” (20 % of ethanol mass fraction) from the critical point. The effect is typically seen at all compositions. In this example, the gradient established is only five times stronger when approaching the critical point.

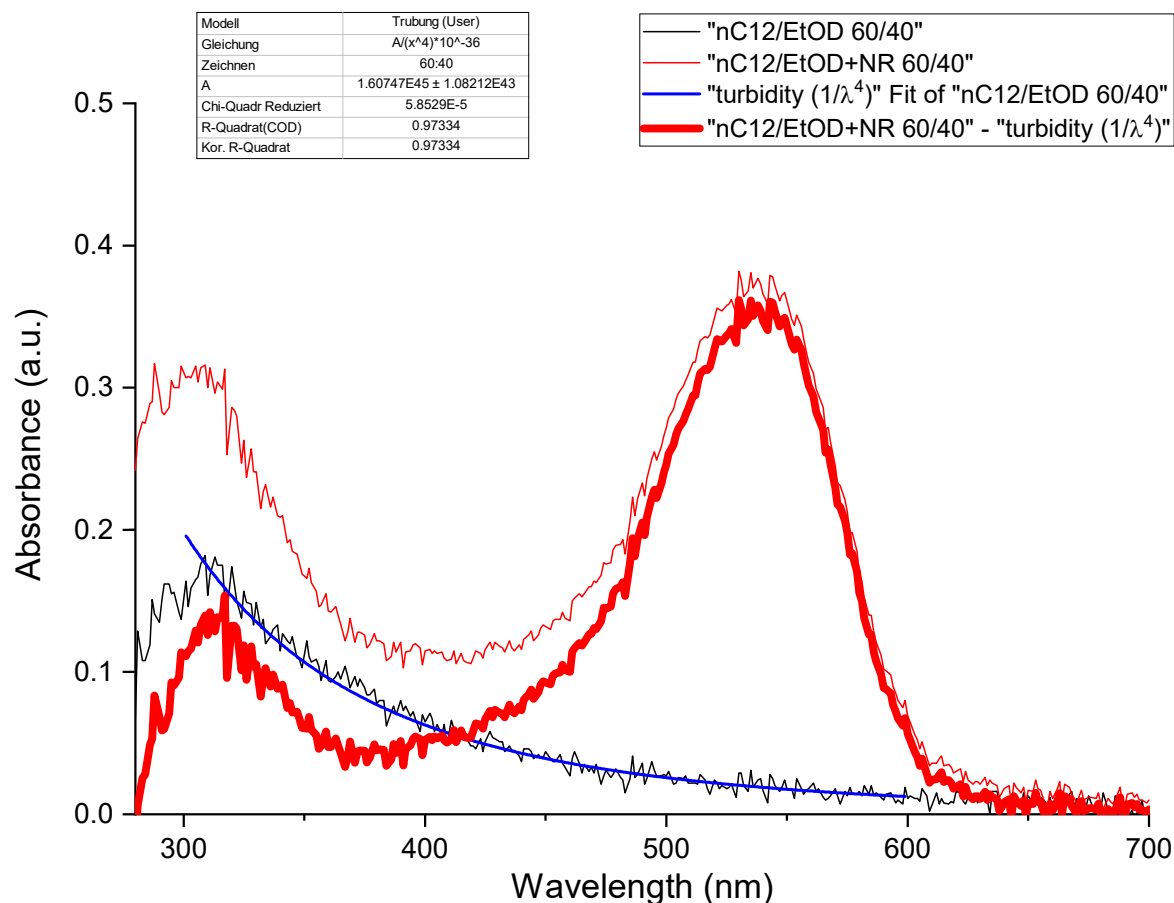


Figure S5: Absorbance observed with (thin red curve) and without (black curve) Nile red dye present: Even in the absence of dye the sample has significant absorption caused by Rayleigh scattering on the large fluctuating domains in the turbid sample that are characteristic of hetero-phase pre-transition fluctuations. The characteristic λ^4 wavelength dependent scattering) overlaps with the UV/Vis absorption spectra of the dye, which can be obtained by subtraction of the λ^4 fit (blue curve) from the absorbance in the presence of the dye. The resulting UV/Vis absorption spectra of the dye is shown in thick red.

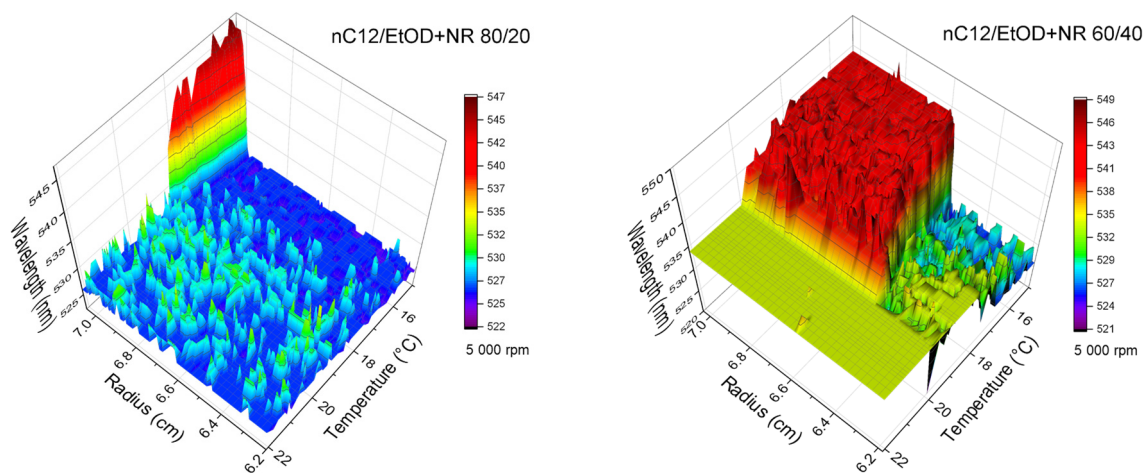


Figure S6: The same data as in figure 3, but plotted as the wavelength of the maximum of the absorption spectra. This demonstrates that there are small negligible variations in the molecular environment of the dye, according to the theories of A. Ben Naim¹ and R Piazza².

¹ A. Ben Naim *Solvation Thermodynamics*, Springer, 1987

² E. Lattuada, S. Buzzaccaro, and R. Piazza PRL 116, 038301 (2016)

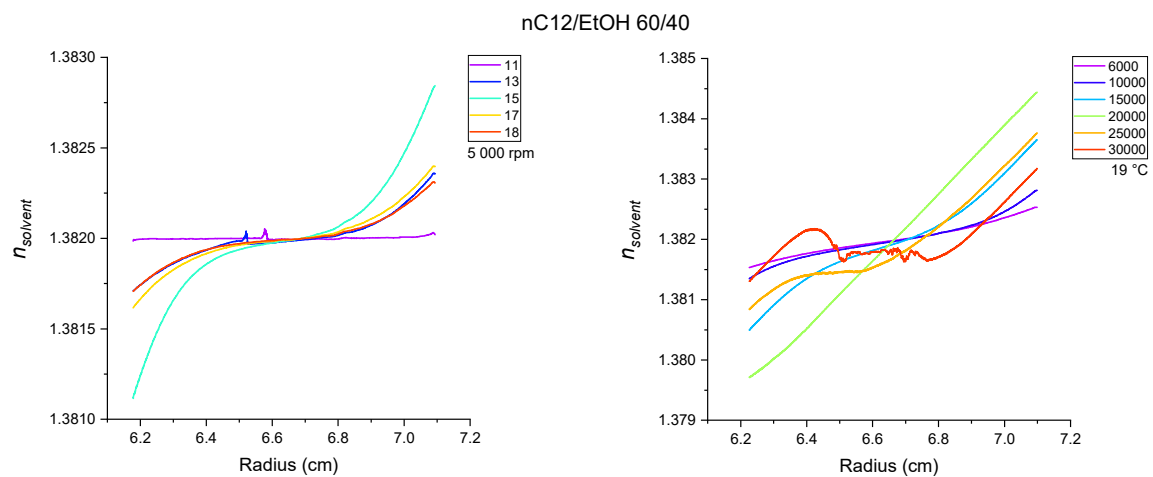


Figure S7: The same experiments as shown in figures 3 and 4, but now the y-scale is expressed in refractive index instead of ethanol volume fraction.

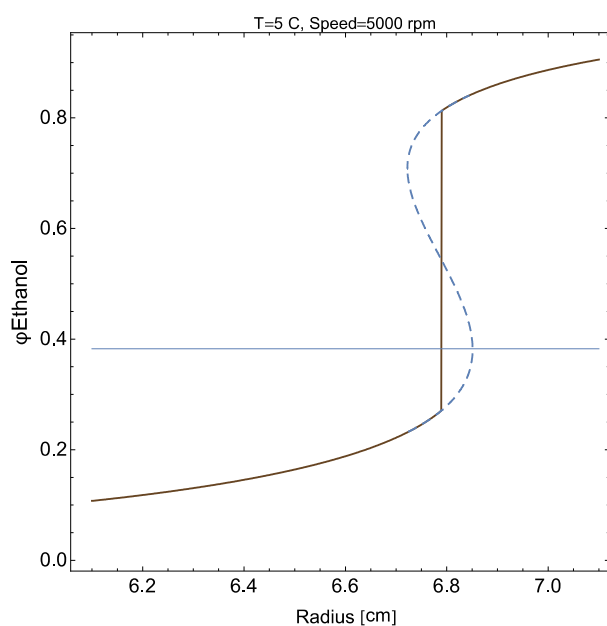


Figure S8: Method of determination of the location of phase transition. Below the critical temperature we use the Maxwell construction, which preserves the total composition of the sample. The method is similar to the evaluation of the partition for lamellar phases³. At the critical temperature the position of the transition varies with the composition of the sample but does not appreciably change in shape. The critical isotherms resemble the Van der Waals critical isotherm.

³ Th Zemb et al., “Osmotic Pressure of Highly Charged Swollen Bilayers,” in *Trends in Colloid and Interface Science*, vol. 89, Progress in Colloid & Polymer Science, (Darmstadt: Steinkopff, 1992), 33–38, doi:10.1007/BFb0116272.

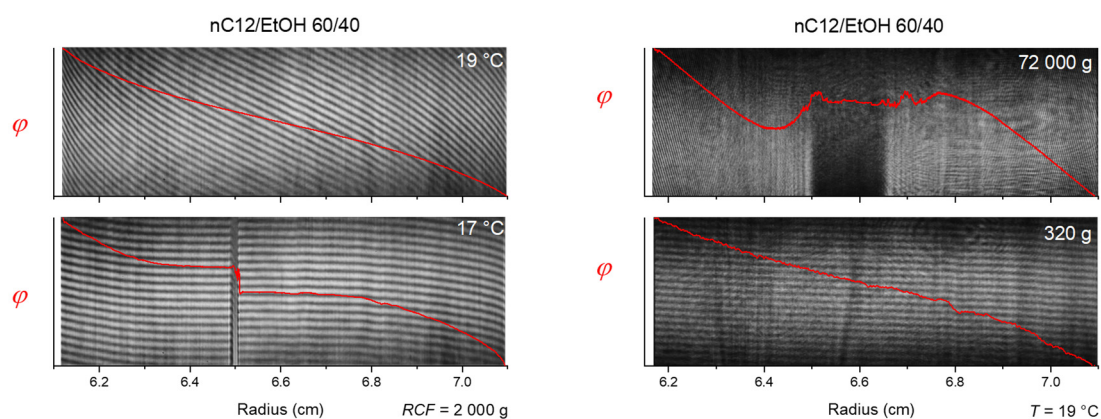


Figure S9: Overlay of fringe patterns and composition profiles close to the critical point. Left: temperature variation at a constant relative centrifugal force ($RCF = \omega^2 r/g$). Right: speed variation at a constant temperature. The red line indicates the Fourier transformed refractive index difference gradient.

Determination of phase transition temperature of ethanol(+Nile red)/dodecane mixtures



Figure S10: Image of the complete equipment setup for the determination of the binary phase diagram (BPD) at the University of Konstanz (UniKon). (A) Water/ethylene glycol bath with a precision Pt100 temperature sensor. (B) Refrigerated Circulator F26 (JULABO GmbH, Germany). (C) Laptop with a LabVIEW program (LabVIEW 2018, 32 bit from National Instruments) to read out the temperature of the water/ethylene glycol bath. (D) Canon EOS 6D camera to take an image of the mixtures in 0.1 °C steps.

Table S1: Video links show the images of the single phase to two phases transition temperature of ethanol(+Nile red)/n-dodecane mixtures, which were performed in 0.1 °C temperature interval during slow cooling by the apparatus setup in Figure S10. The current ethanol mass fraction and temperature are displayed.

Ethanol mass fraction	Video link
ethanol/n-dodecane binary mixtures	
0.225, 0.250, 0.275 and 0.300	https://youtu.be/jH1g5aVyYTI
0.325, 0.350, 0.375 and 0.400	https://youtu.be/oA5BUNI9k4U
0.425, 0.450, 0.475 and 0.500	https://youtu.be/ULld6X0EvYI
0.150, 0.200, 0.550 and 0.600	https://youtu.be/5_-uKzF_EWM
ethanol+Nile red/n-dodecane binary mixtures	
0.225, 0.250, 0.275 and 0.300	https://youtu.be/5j2z_VjnKoU
0.325, 0.350, 0.375 and 0.400	https://youtu.be/F3DRYKB1_C4
0.425, 0.450, 0.475 and 0.500	https://youtu.be/zL-ndyUss3M
0.150, 0.200, 0.550 and 0.600	https://youtu.be/491QOVeqIM

Calculating ε and c for Nile red from Ultraviolet-visible absorption spectra⁴

UV-visible light absorption was used as detection method. The total absorbance of Nile red in solution of two different solvents at any given wavelength can be calculated directly from the AUC absorbance measurement using Lambert-Beer's law:

$$A_{M,\lambda} = A_{E,\lambda} + A_{D,\lambda} = \varepsilon_{E,\lambda} * c_E * a + \varepsilon_{D,\lambda} * c_D * a \quad (1)$$

where A is the total absorbance, ε is the molar extinction coefficient in $\text{L mol}^{-1} \text{cm}^{-1}$ and c is the molar concentration of Nile red in the appropriate solvent, a is the optical path length in centimeters. The subscripts refer to the corresponding solvents, M is mixture, D is dodecane and E is D-ethanol. The UV/Visible absorbance spectra of Nile red in the used solvents are shown in Fig. S11 as an AUC scan in wavelength viewer mode at a single radial position.

From equation (1) it is possible to calculate the concentration of Nile red in the individual solvent phase of a mixture. It is only necessary to know or determine the molar extinction coefficient of Nile red in these solvents. For this, standard solutions with known concentrations were used and their absorbance was measured in the wavelength region of 200 nm to 900 nm in a 1 cm cuvette using the Varian Cary 50 UV-Visible Spectrophotometer (Varian Inc., Australia). From the plot of the measured absorbance versus the concentration, the determined molar extinction coefficient at each wavelength follows from the slope of the calibration straight. Fig. S12 shows an example of these calibration plots for Nile red in dodecane and D-ethanol at the top and the resulting distributions of the molar extinction coefficients at the bottom.

With the known values of ε and a , equation (1) represents now two unknowns (c_D and c_E) and it can be solved with the analysis of the absorbance of a mixture at two different wavelengths. However, it is important that the selected wavelengths are ones at which the molar absorption properties of the two solvents differ significantly. Thus,

$$A_{M1} = (\varepsilon_{E1} c_E + \varepsilon_{D1} c_D) a \quad (2)$$

$$A_{M2} = (\varepsilon_{E2} c_E + \varepsilon_{D2} c_D) a \quad (3)$$

here the subscript 1 describes measurement at wavelength λ_1 , and the subscript 2 describes measurement at wavelength λ_2 . From equation (2), the following equation holds:

$$c_E = \frac{A_{M1}/a - \varepsilon_{D1} c_D}{\varepsilon_{E1}} \quad (4)$$

The molar concentration of Nile red in dodecane can be derived by substituting c_E from equation (4) into equation (3):

$$A_{M2}/a = (\varepsilon_{E2} \frac{A_{M1}/a - \varepsilon_{D1} c_D}{\varepsilon_{E1}} + \varepsilon_{D2} c_D)$$

$$\frac{A_{M2}}{a} - \frac{\varepsilon_{E2} A_{M1}}{\varepsilon_{E1} a} = c_D \left[\frac{\varepsilon_{E1} \varepsilon_{D2} - \varepsilon_{E2} \varepsilon_{D1}}{\varepsilon_{E1}} \right]$$

⁴ Kortüm G Kolorimetrie, Photometrie und Spektrometrie: eine Anleitung zur Ausführung von Absorptions-, Emissions-, Fluoreszenz-, Streuungs-, Trübungs- und Reflexionsmessungen. Springer, Berlin, 1962.

$$c_D = \frac{1}{a} \left[\frac{\varepsilon_{E1} A_{M2} - \varepsilon_{E2} A_{M1}}{\varepsilon_{E1}} \right] \left[\frac{\varepsilon_{E1}}{\varepsilon_{E1} \varepsilon_{D2} - \varepsilon_{E2} \varepsilon_{D1}} \right] = \frac{1}{a} \left[\frac{\varepsilon_{E1} A_{M2} - \varepsilon_{E2} A_{M1}}{\varepsilon_{E1} \varepsilon_{D2} - \varepsilon_{E2} \varepsilon_{D1}} \right] \quad (5)$$

The molar concentration of Nile red in D-ethanol can be derived by substituting c_D from equation (5) into equation (4):

$$c_E = \frac{1}{\varepsilon_{E1}} \left[\frac{A_{M1}}{a} - \varepsilon_{D1} \frac{1}{a} \frac{\varepsilon_{E1} A_{M2} - \varepsilon_{E2} A_{M1}}{\varepsilon_{E1} \varepsilon_{D2} - \varepsilon_{E2} \varepsilon_{D1}} \right] =$$

$$\frac{1}{\varepsilon_{E1} a} \left[\frac{\varepsilon_{E1} \varepsilon_{D2} A_{M1} - \varepsilon_{E2} \varepsilon_{D1} A_{M1} - \varepsilon_{E1} \varepsilon_{D1} A_{M2} + \varepsilon_{E2} \varepsilon_{D1} A_{M1}}{\varepsilon_{E1} \varepsilon_{D2} - \varepsilon_{E2} \varepsilon_{D1}} \right] = \frac{1}{\varepsilon_{E1} a} \left[\frac{\varepsilon_{E1} \varepsilon_{D2} A_{M1} - \varepsilon_{E1} \varepsilon_{D1} A_{M2}}{\varepsilon_{E1} \varepsilon_{D2} - \varepsilon_{E2} \varepsilon_{D1}} \right]$$

Rearrangement leads to:

$$c_E = \frac{1}{a} \left[\frac{\varepsilon_{D2} A_{M1} - \varepsilon_{D1} A_{M2}}{\varepsilon_{E1} \varepsilon_{D2} - \varepsilon_{E2} \varepsilon_{D1}} \right], \text{ and} \quad (6)$$

$$c_D = \frac{1}{a} \left[\frac{\varepsilon_{E1} A_{M2} - \varepsilon_{E2} A_{M1}}{\varepsilon_{E1} \varepsilon_{D2} - \varepsilon_{E2} \varepsilon_{D1}} \right]$$

As can be seen from these relationships, the two wavelengths must be chosen appropriately so that the difference in the denominator becomes as large as possible in order to achieve the greatest accuracy of the concentration determination. Thus,

$$\frac{\varepsilon_{E1}}{\varepsilon_{E2}} \gg \frac{\varepsilon_{D1}}{\varepsilon_{D2}} \quad (7)$$

According to this equation and the molar extinction coefficient distributions in Fig. S12, the wavelengths 560 and 490 nm were chosen for the concentration calculation. Figure 3a-d shows the calculated concentration of Nile red in the dodecane and D-ethanol phase.

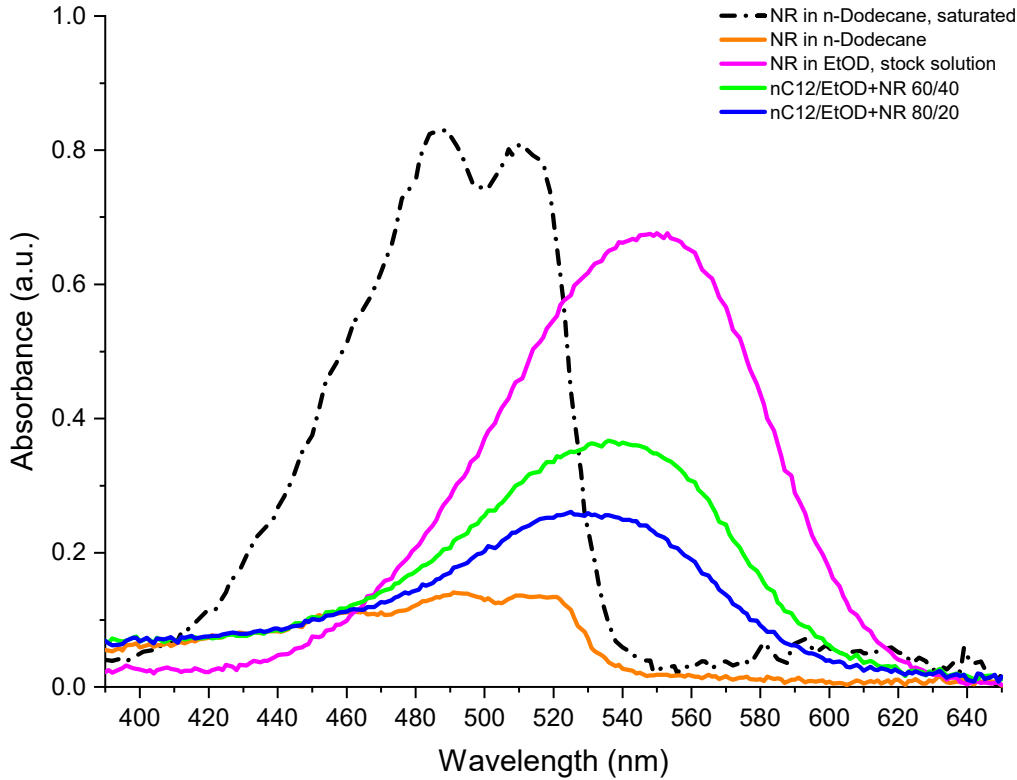


Figure S11: Ultraviolet absorbance spectra for Nile red in dodecane (dot line), in D-ethanol (dot and dash line) and in both solvent mixtures (solid line) collected in an AUC cell ($a = 1.2$ cm).

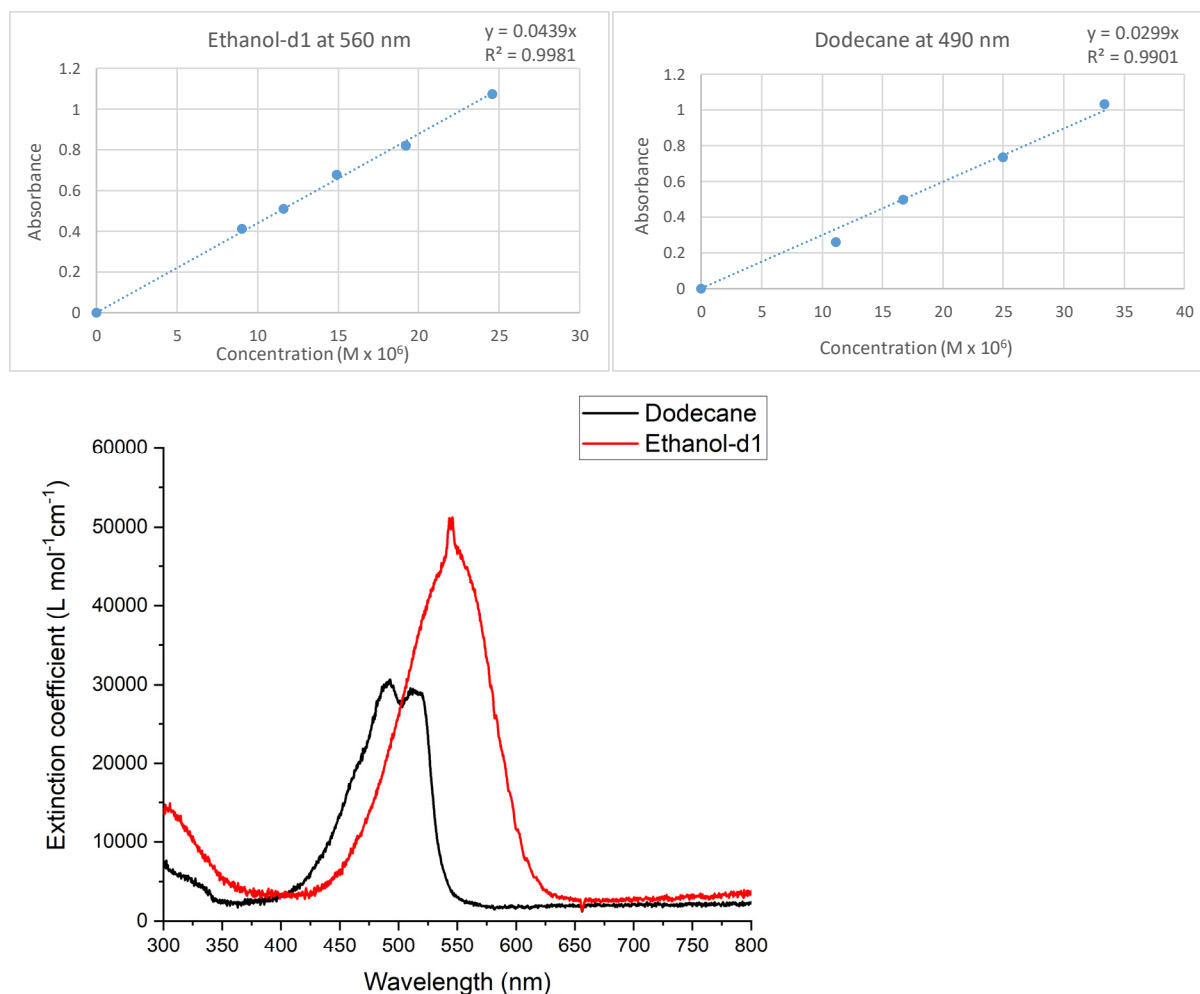


Figure S12: A demonstration of a calibration curves for Nile red in D-ethanol and dodecane on the top and the resulting distributions of the molar extinction coefficients on the bottom.

Derivation of Equation 10 from Density Functional Theory

Consider the free energy of the system given as a density functional $\mathcal{F}[\{\rho_i(\mathbf{r})\}]$. Within the local density approximation (LDA) :

$$\mathcal{F}[\{\rho_i(\mathbf{r})\}] = \iiint f(\{\rho_i(\mathbf{r})\}) d\mathbf{r} + \iiint \sum_i m_i \rho_i(\mathbf{r}) \psi_G d\mathbf{r}.$$

The external potential reads $\psi_G = gz$ in a vertical gravitational field $\mathbf{g} = -g\mathbf{e}_z$ where \mathbf{e}_z is a unit vector of the vertical component z . For centrifugation, we have $\psi_G = -\frac{\omega^2 r^2}{2}$ (in cylindrical coordinates) and $\mathbf{g} = \omega^2 r \mathbf{e}_r$ where \mathbf{e}_r is a unit vector of the radial component r . $f(\{\rho_i(\mathbf{r})\})$ is the free energy per unit of volume of the mixture when the temperature T is fixed. We considered the Flory-Huggins expression for the numerical calculations presented here but any model can be used. Considering the Gibbs-Duhem equation, we have $f(\{\rho_i(\mathbf{r})\}) = \sum_i \mu_i \rho_i(\mathbf{r}) - P$. The chemical potentials μ_i and the pressure P depend on the position \mathbf{r} via the number densities $\{\rho_i(\mathbf{r})\}$.

Let us find the free energy minimum with the condition of constant number of particles:

$$\iiint \rho_i(\mathbf{r}) d\mathbf{r} = N_i^{\text{tot}}$$

For any i , we have $\frac{\delta \mathcal{F}}{\delta \rho_i(\mathbf{r})} - \lambda_i = 0$ where λ_i is the Lagrange multiplier associated to the i^{th} conservation equation. Hence

$$\sum_i \left(\mu_i(\mathbf{r}) + \rho_i(\mathbf{r}) \frac{\partial \mu_i}{\partial \rho_i}(\mathbf{r}) - \frac{\partial P}{\partial \rho_i}(\mathbf{r}) + m_i \psi_G - \lambda_i \right) = \sum_i (\mu_i(\mathbf{r}) + m_i \psi_G - \lambda_i) = 0$$

where we used the Gibbs-Duhem equation (at constant temperature). The latter equation expresses the fact that the chemical potential is constant in the system (chemical equilibrium). The gravitational force simply adds a gravitational contribution $m_i \psi_G$ to μ_i . The added term is similar to the concept of electro-chemical potential $\mu_i + q_i \psi$ in electrochemistry (q_i is the charge of i and ψ the electric potential). The Lagrange multiplier λ_i is nothing but this generalized chemical potential $\tilde{\mu}_i = \mu_i + m_i \psi_G$.

The distribution profile at equilibrium can be calculated from this condition: $\tilde{\mu}_i$ is constant anywhere in space. The formula can be explicitated by taking the gradient:

$$\mathbf{grad} \mu_i = \frac{\partial \mu_i}{\partial P} \mathbf{grad} P + \mathbf{grad}_P \mu_i = -m_i \mathbf{grad} \psi_G = m_i \mathbf{g}$$

with \mathbf{grad}_P is the gradient calculated at constant pressure (contribution due to the composition gradient). Thanks to Gibbs-Duhem $\mathbf{grad} P = -\sum_i \rho_i \mathbf{grad} \mu_i = \sum_i m_i \rho_i \mathbf{g}$.

The partial volume of i is $V_i = \frac{\partial V}{\partial N_i} = \frac{\partial \mu_i}{\partial P}$. We obtain

$$V_i \sum_j m_j \rho_j \mathbf{g} + \mathbf{grad}_P \mu_i = m_i \mathbf{g}$$

so that

$$\mathbf{grad}_P \mu_i = \left(m_i - V_i \sum_j m_j \rho_j \right) \mathbf{g}$$

This is the most general equation. The second term represents a kind of buoyant force (Archimedes principle).

A general way to write the chemical potential is

$$\mu_i(T, P, \{x_i\}) = \mu_i^*(T, P) + k_B T \ln(x_i \gamma_i)$$

Rigorously, without neglecting their pressure dependence, the activity coefficients γ_i depend on T , P , and $\{x_i\}$. $\mu_i^*(T, P)$ is the chemical potential of pure i . In order to apply this expression in terms of molar fractions x_i into the general expression, the number densities ρ_j can be expressed as functions of x_i thanks to the partial volumes:

$$\rho_j = \frac{n_j}{\sum_k n_k V_k} = \frac{x_j}{\sum_k x_k V_k}$$

Then the distribution profiles follow:

$$k_B T \mathbf{grad}_P \ln(x_i \gamma_i) - \left(m_i - \frac{V_i \sum_j x_j m_j}{\sum_k x_k V_k} \right) \mathbf{g} = 0$$

The calculation is practically complicated because partial volumes depend on the composition, but the dependence is usually very weak and can be neglected in a first approach.

Then the practical calculation requires the knowledge of the activity coefficients γ_i . The simplest model of non-ideal binary mixtures is the Hildebrand regular solution model for which

$$\gamma_1 = e^{\alpha x_2^2} \quad \text{and} \quad \gamma_2 = e^{\alpha x_1^2}$$

The Hildebrandt parameter $\alpha = \frac{q}{k_B T} \left(E_{AB} - \frac{1}{2} (E_{AA} + E_{BB}) \right)$ is positive for repulsive solution (for which there is a tendency to demix) and negative for an attractive solution (for which mixture is energetically favorable). q is the number of neighbours for any molecules and $E_{\alpha\beta}$ are interaction energies. Furthermore, we consider that $V_1 = V_2$. In that case

$$m_i^{\text{eff}} = m_i - \frac{V_i \sum_j x_j m_j}{\sum_k x_k V_k} = (1 - x_i)(m_i - m_j)$$

where $j = 2$ if $i = 1$ and $j = 1$ if $i = 2$. In the radial direction, the profile equation applied to x_1 becomes:

$$k_B T \frac{d}{dr} (\ln x_i + \alpha (1 - x_1)^2) - (1 - x_1)(m_1 - m_2) \omega^2 r = 0$$

so that

$$k_B T \left(\frac{1}{x_1} - 2\alpha(1 - x_1) \right) \frac{dx_1}{dr} - (1 - x_1)(m_1 - m_2)\omega^2 r = 0$$

The solution of the differential equation $x_1(r)$ can be found by the separation of variables method. We obtain:

$$\ln \frac{x_1}{1 - x_1} - 2\alpha x_1 = \frac{(m_1 - m_2)\omega^2 r^2}{2k_B T} + A$$

The integration constant A is such that the conservation of particles in the column is obtained. In the model with the same constant partial volumes for the two species, the local total number density is constant:

$$\rho_1(\mathbf{r}) + \rho_2(\mathbf{r}) = x_1(\mathbf{r})\rho_{\text{tot}}(\mathbf{r}) + (1 - x_1(\mathbf{r}))\rho_{\text{tot}}(\mathbf{r}) = \rho_{\text{tot}}(\mathbf{r}) = \rho_{\text{tot}}.$$

So the condition for $x_1(\mathbf{r})$ is:

$$\iiint x_1(\mathbf{r})\rho_{\text{tot}} \, d\mathbf{r} = N_1^{\text{tot}} = \bar{x}_1 N^{\text{tot}} = \bar{x}_1 \iiint \rho_{\text{tot}} \, d\mathbf{r}$$

Thus, the value of A is obtained from conservation of the average molar fraction:

$$\iiint x_1(\mathbf{r}) \, d\mathbf{r} = \bar{x}_1 \iiint d\mathbf{r} = \bar{x}_1 V$$

The Flory-Hugginsⁱ theory is an extension of regular solution theory in which the second component is identified as a polymer for which the size is r^{FH} times bigger than the one of the solvent. The activities read

$$\ln a_1 = \ln x_1 \gamma_1 = \ln \phi_1 + \left(1 - \frac{1}{r^{FH}} \right) \phi_2 + \chi \phi_2^2$$

$$\ln a_2 = \ln x_2 \gamma_2 = \ln \phi_2 - (r^{FH} - 1)\phi_1 + \chi r^{FH} \phi_1^2$$

Following the same procedure with $V_1 = v_0$ and $V_2 = r^{FH} v_0$ we get eq. (10). It should be noted that this formalism can be applied for any mixture. It allows Tsori and Leibler's work to be generalised to any binary system whose equation of state (Gibbs energy or activity coefficients) is known. It also makes it possible to understand how the pressure gradient is coupled to the action of the external field by imposing buoyancy. Finally, it can be easily generalized to calculate the temporal evolution by a TDDFT formalism.

ⁱ J. M. Prausnitz, R. M. Lichtenthaler and E. G. de Azevedo *Molecular thermodynamics of fluid phase equilibria*, Prentice Hall, 1985.